Journal Pre-proofs

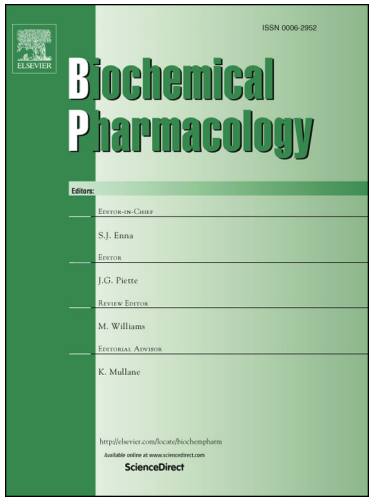

Andrographolide inhibits inflammatory responses in LPS-stimulated macrophages and murine acute colitis through activating AMPK

Nami Kim, Peeraphong Lertnimitphun, Yiwen Jiang, Hongsheng Tan, Hua Zhou, Yue Lu, Hongxi Xu

PII: S0006-2952(19)30345-4
DOI: https://doi.org/10.1016/j.bcp.2019.113646
Reference: BCP 113646

To appear in: *Biochemical Pharmacology*

Received Date: 9 August 2019
Accepted Date: 19 September 2019

Please cite this article as: N. Kim, P. Lertnimitphun, Y. Jiang, H. Tan, H. Zhou, Y. Lu, H. Xu, Andrographolide inhibits inflammatory responses in LPS-stimulated macrophages and murine acute colitis through activating AMPK, *Biochemical Pharmacology* (2019), doi: https://doi.org/10.1016/j.bcp.2019.113646

Andrographolide inhibits inflammatory responses in LPS-stimulated macrophages and murine acute colitis through activating AMPK

Nami Kim [a,1], Peeraphong Lertnimitphun [a,1], Yiwen Jiang [a], Hongsheng Tan [a], Hua Zhou [b], Yue Lu [a#], Hongxi Xu [a, b#]

[a] School of Pharmacy, Shanghai University of Traditional Chinese Medicine, Shanghai, 201203, People's Republic of China

[b] Institute of Cardiovascular Disease of Integrated Traditional Chinese and Western Medicine, Shuguang Hospital, Shanghai University of Traditional Chinese Medicine, Shanghai, 201203, People's Republic of China

[#] Correspondence should be addressed to:

Hongxi Xu, School of Pharmacy, Shanghai University of Traditional Chinese Medicine, Shanghai 201203, PR China. Tel: 86-21-51323089, Fax: 86-21-51323089, E-mail address: xuhongxi88@gmail.com.

Or: Yue Lu, School of Pharmacy, Shanghai University of Traditional Chinese Medicine, Shanghai 201203, PR China. Tel: 86-21-51322026, E-mail address: lvyue126@hotmail.com

[1] These authors contributed equally to this work

ABSTRACT

Andrographolide (Andro), a well-known labdane diterpenoid of *Andrographis paniculata*, has been reported to have anti-inflammatory effects in various inflammatory disease models. Despite ongoing efforts to elucidate the anti-inflammatory mechanism of Andro, its specific mechanism is not entirely clear. In this study, we confirmed the inhibitory effect of Andro on inflammatory activity and studied its mechanism in depth to find potential anti-inflammatory targets of Andro using lipopolysaccharide (LPS)-induced macrophages *in vitro* and a dextran sulfate sodium (DSS)-induced mouse model of acute colitis *in vivo*. We found that Andro significantly reduced proinflammatory cytokines by suppressing nuclear factor kappa B (NF-κB), mitogen-activated protein kinase (MAPK) and their upstream signaling pathways and activating the AMP activated protein kinase (AMPK) pathway in LPS-induced macrophages. Interestingly, Andro could not regulate the activation of the AMPK/NF-κB/MAPK pathway nor inhibit NF-κB and activator protein 1 (AP-1) nuclear translocation and nitric oxide (NO) production following knockdown of AMPKα2. Moreover, Andro attenuated DSS-induced intestinal barrier dysfunction and inflammation by suppressing the NF-κB and MAPK pathways in colon tissues while activating the AMPK pathway. In conclusion, our study demonstrates that Andro effectively inhibits LPS-induced inflammatory responses via AMPK activation in macrophages, whereby Andro can ameliorate DSS-induced acute colitis in mice.

Keywords: Andrographolide, AMPK, Inflammation, Macrophage, Acute colitis

Abbreviations: AMPK, AMP activated protein kinase; Andro, Andrographolide; AP-1, activator protein-1; CD, Crohn's disease; COX-2, cyclooxygenase-2; DSS, dextran sulfate sodium; ERK, extracellular signal regulated kinase; IBD, inflammatory bowel disease; IκBα, nuclear factor of kappa light polypeptide gene enhancer in B-cells inhibitor, alpha; IKKα/β, IκB kinase α/β; IL, Interleukin; iNOS, inducible nitric oxide synthase; JNK, c-Jun NH_2-terminal kinase; LPS, lipopolysaccharide; MAPK, mitogen-activated protein kinase; NF-κB, nuclear factor kappa B; NO, nitric oxide; SASP, sulfasalazine; siRNA, small interference ribonucleic acid; TLR4, Toll-like receptor 4; TNF-α, tumor necrosis factor-α; UC, ulcerative colitis.

1. Introduction

Andrographolide (Andro) is a natural compound isolated from *Andrographis paniculate* (Burm. f.) Nees which has long been used in China, India, and other parts of Asia for the treatment of inflammation-related diseases such as flu, upper respiratory tract infection, diarrhea and dysentery[1-3]. Previous studies have suggested that Andro has a wide range of biological activities including anti-viral[4-6], anti-cancer[7-10] and anti-inflammatory[1, 11-13] effects. Among them, its anti-inflammatory effects have been caused by suppressing NF-κB/MAPK signaling pathway and activating nuclear factor E2-related factor 2 (Nrf2) signaling pathway in LPS- or tumor necrosis factor (TNF)-α-induced immune cells[1, 6], as well as in a variety of inflammatory disease models, such as asthma[14-16], chronic obstructive pulmonary disease (COPD)[17-19], hepatitis[20], inflammatory bowel disease (IBD)[21-24], and so on. Nevertheless, the molecular mechanism underlying the anti-inflammatory properties of Andro is still not fully clear and therefore requires further elucidation.

Macrophages are major immune cells that are regarded as key cellular components in the initiation, maintenance and resolution of inflammation[25]. Activated macrophages by LPS (or LPS and interferon (IFN)-γ) induce innate immune response and produce proinflammatory mediators that lead to inflammation[25]. Therefore, macrophages are targeted as a potential therapeutic intervention for controlling inflammatory diseases, such as inflammatory bowel disease (IBD)[26-28].

IBD, which is composed mainly of ulcerative colitis (UC) and Crohn's disease (CD), represents intestinal inflammatory disorders, although the pathogenesis of IBD still remains unknown; however, it is believed to involve the gut microbiota, environmental and genetic factors that regulate the mucosal immune response and barrier function[29]. In the past several decades, the incidence of IBD has rapidly increased worldwide and even increased the risk of colon cancer[30]. Furthermore, the current drugs for IBD are limited, the rate of sustained remission is low, and some drugs, such as anti-TNF agents,

also increase the risk of severe infection and malignant tumors[31]. Because of the growing need for safe and effective IBD treatment, the potential of natural products for IBD treatment has gained increased attention.

The purpose of the present study was to confirm the anti-inflammatory effect of Andro and investigate the underlying mechanism of Andro-associated inflammation control, which may provide a scientific basis for the future development of anti-inflammatory drugs to treat IBD.

2. Materials and methods

2.1. Chemicals and Reagents

Andrographolide (PubChem CID:5318517) was purchased from Selleckchem (Houston, TX, USA), purity>99% based on HPLC analysis. Dimethyl sulfoxide (DMSO) was the control in the all cell experiments and the final concentration of DMSO was adjusted to 0.1% (v/v) in culture media. DMSO, LPS (*E. coli*, O55 : B5), IFN-γ, MTT, phorbol-12-myristate-13-acetate (PMA) and sulfasalazine (SASP) were purchased from Sigma-Aldrich (St. Louis, MO, USA). DSS (MW: 36,000–50,000 Da) was purchased from MP Biomedicals (Solon, OH, USA). AICAR and Compound C were purchased from Millipore (Billerica, MA, USA). Dulbecco's modified Eagle medium (DMEM), RPMI 1640, and fetal bovine serum (FBS) were purchased from Thermo Fisher Scientific (Grand Island, NY, USA). Penicillin-streptomycin was purchased from GENOM (Hangzhou, China).

2.2. Culture and activation of macrophages

The murine macrophage cell line RAW264.7 was obtained from the Shanghai Institutes for Biological Sciences (SIBC) cell line stock and cultured in DMEM supplemented with 10% heat-inactivated FBS, 100 U/ml penicillin and 100 g/ml streptomycin. The human promonocytic leukemia cell line U937 was maintained in

RPMI 1640 medium with 10% heat-inactivated FBS, 100 U/ml penicillin and 100 g/ml streptomycin. All cell lines were incubated at 37 °C with 5% CO_2 in humidified atmosphere. For differentiation of U937 into macrophages, 1×10^6 U937 cells were incubated for 48 h with 100 ng/ml PMA and then had a resting period of 24 h in the culture medium without PMA. The primary macrophage BMDMs (Bone marrow derived macrophages) from mice were prepared as described previously[32].

2.3. Griess and ELISA assay

RAW264.7 (5×10^5 cells/ml in 12-well plate) cells were pretreated with or without Andro for 1 h and then incubated with or without LPS for 12 h (for ELISA assay) or 24 h (for Griess assay). After cell culture supernatants were collected, NO production was determined by measuring nitrite content using the Griess Reagent System (Promega, Madison, WI, USA). Interleukin (IL)-6, TNF-α and IL-1β concentrations were determined using Duo Set ELISA Kits (R&D Systems, Minneapolis, MN, USA). The experiment was conducted following the manufacturer's instructions.

2.4. Quantitative real-time PCR

The total RNA of RAW264.7 cells or colon tissues was isolated using RNAiso Plus (TaKaRa, Mountain View, CA, USA) according to the manufacturer's instructions. After the concentration of RNA was measured by spectrophotometer (DeNovix, Wilmington, DE, USA), 1 μg of RNA was reverse transcribed into cDNA using the PrimeScript RT Reagent Kit (TaKaRa, Mountain View, CA, USA), and gene amplification was detected by SYBR-based quantitative PCR analysis (SYBR Green Real-time PCR Master Mix, TOYOBO, Osaka, Japan). The PCR cycles were as follows: 95 °C for 10 min, followed by 40 cycles of 95 °C for 15 s and 60°C for 1 min. The results were analyzed using the $2^{-\Delta\Delta Ct}$ method. The relative gene expression was normalized to β-actin (for RAW264.7 cells) or GAPDH (for colon tissues) expression. The following primers (Generay Biotech, Shanghai, China) were used in the reaction:

IL-6 (mouse) forward: 5'-CTGCAAGAGACTTCCATCCAGTT-3', reverse: 5'-

GAAGTAGGGAAGGCCGTGG-3'; TNF-α (mouse) forward: 5'-CGAGTGACAAGCCTGTAGC-3', reverse: 5'-GGTGTGGGTGAGGAGCACAT-3'; IL-1β (mouse) forward: 5'-ATGTGCTGCTGCGAGATTTGA-3', reverse: 5'-TGCCACCTTTTGACAGTGATG-3'; β-actin (mouse) forward: 5'-GTATGGAATCCTGTGGCATC-3', reverse: 5'-CGTACTCCTGCTTGCTGATC-3'; GAPDH (mouse) forward: 5'-AAATCCCATCACCATCTTCC-3', reverse: 5'-TCACACCCTGACGAACA-3.

2.5. Western blotting

Protein extraction, Western blotting, and densitometry were performed as described previously[33]. The following anti-bodies were used for Western blot analysis: iNOS, COX-2, phospho-IKKα/β, IKKα/β, phospho-IκBα, IκBα, phospho-ERK1/2, ERK1/2, phospho-JNK, JNK, phospho-p38, p38, MyD88, phosphor-IRAK4, IRAK4, β-actin, p65, phospho-c-Jun, c-Fos, β-tubulin, phospho-AMPKα, AMPKα, phospho-LKB1, phospho-ACC, phospho-Akt, phospho-mTOR, phospho-Bad, phospho-p70S6K, phospho-PRAS40, phospho-GSK3β, phospho-S6RP, phospho-Stat1, Caspase3 (cleaved), phospho-Stat3 (Cell Signaling Technology, Danvers, MA, USA), Toll-like receptor 4 (TLR4) (Santa Cruz Biotechnology, Santa Cruz, CA, USA), Lamin A+C, AMPKα2 (Abcam, Cambridge, England), Peroxidase-Labeled Anti-Rabbit IgG (H+L) Antibody and Peroxidase-Labeled Anti-mouse IgG (H+L) Antibody (KPL, Milford, MA, USA).

2.6. Preparation of nuclear and cytosolic extracts

RAW264.7 and U937 cells (1×10^6 cells/ml) were treated with or without LPS for 30 min. The nuclear and cytosolic extracts of the cells were prepared by the Nuclear and Cytoplasmic Protein Extraction Kit (Beyotime Biotechnology, Shanghai, China) according to the manufacturer's instructions, and then Western blot analysis was performed.

2.7. Immunofluorescence (IF)

RAW264.7 and U937 cells (1×10^5 cells/ml) were seeded on coverslips in 12-well plates and cultured overnight. After drug and LPS treatment, cells were fixed with 4% Paraformaldehyde (Sangon Biotech, Shanghai, China) for 15 min, treated with 0.3% Triton X-100 (BioFroxx, Einhausen, Germany) for 10 min and then blocked with 5% bovine serum albumin (BSA) (Biosharp, Hefei, China) in PBS (Maixin Biotech, Fuzhou, China) for 1 h. After that, they were incubated with different primary antibodies for p65 (1:400), p-c-Jun (1:100) and c-Fos (1:6400) at 4℃overnight. The cells were incubated with FITC-labeled goat anti-rabbit IgG (1:500, Beyotime Biotechnology, Shanghai, China) for 1.5 h at room temperature. The nuclei were stained with 4′,6-diamidino-2-phenylindole (DAPI) (Southern Biotech, Birmingham, AL, USA) for 2 h in the dark. Cell imaging was performed and captured by confocal laser scanning microscope (Olympus Corp., Tokyo, Japan).

2.8. Intracellular signaling array

BMDMs (1×10^6 cells/ml) were treated with or without LPS (10 μg/mL) and IFN-γ (20 ng/ml) for 15 min. The prepared cell lysates were used to detect the indicated cellular proteins and signaling nodes by the PathScan® Intracellular Signaling Array Kit (Cell Signaling Technology, Danvers, MA, USA) according to the manufacturer's instructions.

2.9. Transfection of siRNA

RAW264.7 cells (2×10^5 cells/ml) were cultured for 16 h in serum-free DMEM and transfected with pre-designed Mouse Prkaa2 siRNA (GenePharma, Shanghai , China) or negative control siRNA (GenePharma, Shanghai, China) utilizing si RNA-Mate transfection reagent (GenePharma, Shanghai, China) according to the manufacturer's manuals. The medium was changed 48 h after siRNA transfect ion. The following siRNA duplexes were used in the transfection: AMPKα2 si RNA Sense: 5′-GCUGUGGAUCGCCAAAUUATT-3′, Antisense: 5′-UAAUUUG GCGAUCCACAGCTT-3′; Negative control siRNA Sense: 5′-GCGACGAUCUG

CCUAAGAUdTdT-3′, Antisense: 5′-AUCUUAGGCAGAUCGUCGCdTdT-3′.

2.10. Animals

BALB/c male mice (19±1 g, 6-8 weeks of age) were obtained from Shanghai SLAC Animal Laboratory (Shanghai, China). All mice were kept in a specific pathogen-free (SPF) room under a temperature of 22±1 °C, humidity of 55±5% and a 12/12 h light/dark cycle. All animal experiments were conducted in accordance with the regulations on teaching and research management of the Animal Center of Shanghai University of Traditional Chinese Medicine (SHUTCM) after obtaining the approval of the Animal Experimental Ethics Committee of SHUTCM.

2.11. Establishment of murine acute colitis model

Acute colitis was induced by the oral administration of 3.5% DSS as previously described[34]. BALB/c mice were randomly divided into 5 groups: normal group, DSS model group, Andro low-dose group, Andro high-dose group and sulfasalazine (SASP) positive control group. On day 0 and day 7, mice in the DSS model group, Andro low- and high-dose groups and positive control group were given 3.5% DSS drinking water; the normal group was given sterile water. In our preliminary experiments, we found that the toxicity of Andro *in vivo* was negligible at 200 mg/kg; however, the colonic wall of the 200 mg/kg group became thin, so 50 and 100 mg/kg were selected as the doses for subsequent animal experiments. On days 1-7, the low-dose group of Andro was administered a dose of 50 mg/kg, the high-dose group of Andro was administered a dose of 100 mg/kg, and the SASP positive control group was given a dose of 200 mg/kg. The corresponding dose of Andro or SASP was administered i.g. according to the weight of each mouse; the DSS model group was given PBS. On day 8, the mice were sacrificed and dissected, and colon tissue and spleen cells were collected for subsequent experiments. Sample sizes were n = 4 to 5 per group for all studies.

2.12. Disease activity evaluation, hematoxylin and eosin and immunohistochemistry

Disease activity index (DAI)[35, 36], hematoxylin and eosin (H&E) [37] and immunohistochemistry (IHC) [37] were performed as described previously. Primary antibodies against F4/80 and CD68 (Servicebio, Wuhan, China) were diluted 1:300, and HRP-conjugated Goat Anti-Rabbit antibodies (Servicebio, Wuhan, China) were diluted 1:200 for IHC staining.

2.13. Statistical analysis

Data are presented as the mean ± SD, which were calculated from at least triplicate determinations. GraphPad Prism 5.0 software (La Jolla, CA, USA) was used to calculate and statistically analyze the experimental data. The statistical significance between two groups was determined by unpaired Student's t-test, and multiple comparisons were conducted by one-way ANOVA with Tukey's post hoc test. The results were considered statistically significant when the p value was less than 5%.

3. Results

3.1. Andro inhibits the production of NO and proinflammatory cytokines without affecting cell viability

First, we detected the cytotoxic effects of Andro on RAW264.7 cells (Fig. 1A) using the MTT assay and found that Andro did not significantly affect cell viability at concentrations ranging from 1 to 10 μM. Therefore, the concentration of Andro was no more than 10 μM in subsequent experiments. To investigate the anti-inflammatory effect of Andro, we determined NO production and iNOS and COX-2 protein expression in LPS-stimulated macrophages. As expected, NO production (Fig. 1B) and iNOS and COX-2 protein expression (Fig. 1D) were markedly increased by LPS stimulation in RAW264.7 cells; by contrast, Andro inhibited them in a dose-dependent manner. Similar results were obtained from primary murine macrophage BMDMs (Fig. 1C and 1E).

Next, we determined whether Andro affected proinflammatory cytokines, which increased the inflammatory response in LPS-stimulated RAW264.7 cells. The secretion and mRNA levels of IL-6, TNF-α and IL-1β were measured by ELISA and RT-PCR. LPS significantly increased the secretion (Fig. 1F) and mRNA levels (Fig. 1G) of IL-6, TNF-α and IL-1β in the control group, but Andro decreased the expression of these cytokines in a dose-dependent manner.

3.2. Andro inhibits the activation of NF-κB/MAPK/TLR4-MyD88 signaling pathways in LPS-stimulated macrophages

We next evaluated the effect of Andro on LPS-induced NF-κB, MAPK and their upstream signaling pathway, which are known as classical inflammatory pathways to mediate the production of proinflammatory cytokines. Andro suppressed the phosphorylation of IKKα/β, IκBα, ERK1/2, JNK, p38 and IRAK4 in a dose-dependent manner. Additionally, the degradation of IκBα and the activation of TLR4 and MyD88 were inhibited by Andro in LPS-stimulated RAW264.7 (Fig. 2A), BMDM (Fig. 2B) and U937 (data not shown) cells. These Western blot results clearly demonstrate that Andro is capable of inhibiting the LPS-induced NF-κB, MAPK and TLR4-MyD88 signaling pathways.

3.3. Andro inhibits NF-κB p65 and AP-1 nuclear translocation in LPS-stimulated macrophages

To investigate the effect of Andro on NF-κB p65 and AP-1 nuclear translocation, we performed measurements using Western blotting and IF. As shown in Western blot analysis, when RAW264.7 (Fig. 3A) and U937 (data not shown) cells were stimulated by LPS, Andro treatment significantly decreased the p-c-Jun and c-Fos protein levels in both the cytoplasm and nucleus. Moreover, IF analysis also showed that Andro significantly suppressed the nuclear translocation of p65, p-c-Jun and c-Fos in LPS-stimulated RAW264.7 (Fig. 3B) and U937 (data not shown) cells. These results indicate that Andro inhibits the nuclear translocation of the transcription factors NF-κB and AP-

1 in LPS-stimulated macrophages.

3.4. Andro activates the AMPK pathway in LPS-induced macrophages

To further investigate the specific anti-inflammatory mechanisms and potential molecular targets of Andro, we used an intracellular signal array kit and Western blotting to detect the expression of some specific proteins related to cell growth, metabolism, apoptosis, etc., in LPS-induced BMDM and RAW264.7 cells (Fig. 4). The results of the intracellular signal array kit showed that the cleaved Caspase-3 protein level and the phosphorylation of Stat1, Stat3, Akt, AMPKα, S6 Ribosomal Protein (S6RP), mTOR, HSP27, Bad, p70S6K, p53, PRAS40, p38, SAPK/JNK, PARP and GSK3β on BMDMs were upregulated following LPS treatment (Fig. 4A and B). Similar results were observed in RAW264.7 cells (Fig. 4C and D). However, the level of AMPKα phosphorylation was significantly increased in BMDMs following LPS treatment, but there was no significant change in Raw264.7 cells. In addition, Andro not only reduced the cleaved Caspase-3 protein level and the phosphorylation of Akt, mTOR, Bad, p70S6K, PRAS40, S6RP, Stat1 and Stat3 but also significantly increased the phosphorylation of LKB1, AMPKα, ACC, and GSK3β in LPS-induced RAW264.7 cells. We also detected the expression levels of procaspase-3 and the respective total protein of Fig. 4C and 4D and then normalized to β-actin, there were no differences between the relative protein levels of each group (data not shown). These finding suggest that Andro has a therapeutic effect on specific proteins involved in inflammation, metabolism and apoptosis, especially those involved in regulating the AMPK pathway.

3.5. AMPK activation is associated with the inhibitory effect of Andro on LPS-induced NF-κB/MAPK pathways

In a recent study, AMPK activation was considered to participate in anti-inflammatory functions in macrophages by inhibiting the NF-κB and MAPK signaling pathways[38]. To further validate the role of AMPK in the anti-inflammatory mechanism

of Andro, we compared the inhibitory effect of Andro with those of the AMPK activator AICAR and AMPK inhibitor Compound C for the AMPK, NF-κB and MAPK pathways in LPS-induced RAW264.7 cells. In the AMPK signaling pathway, Andro and AICAR both activated the phosphorylation of the LKB1, AMPKα, ACC and GSK3β proteins and also inhibited the phosphorylation of mTOR and p70S6K (Fig. 5A). Simultaneously, Andro inhibited the degradation of IκBα and the phosphorylation of the IKKα/β, IκBα, ERK, JNK and p38 proteins in the NF-κB and MAPK signaling pathways (Fig. 5B and C). AICAR also inhibited the phosphorylation of IκBα and the degradation of IκBα but had no significant inhibitory effect on the phosphorylation of IKKα/β, ERK, JNK and p38 protein levels. Compound C did not affect the activation of the AMPK/NF-κB/MAPK pathways. These results show that AMPK activation may be involved in the inhibitory effects of Andro on the NF-κB and MAPK pathways in LPS-induced macrophages.

3.6. AMPKα2 knockdown reduces the anti-inflammatory functions of Andro

To further investigate whether the anti-inflammatory effects of Andro are dependent or independent of AMPK, we used siRNA transfection for AMPKα2 gene silencing in RAW264.7 cells. In our study, we observed that Andro significantly inhibited LPS-induced NO production in the negative control group but not in AMPKα2-knockdown macrophages (Fig. 6A). We next evaluated the effects of Andro on LPS-induced AMPK/NF-κB/MAPK signaling pathways following AMPKα2 knockdown. Andro-induced LKB1 phosphorylation was not affected by AMPKα2 knockdown. However, the Andro and AICAR-induced p-AMPKα upregulation were reduced by 80-90% following AMPKα2 knockdown ($P < 0.05$). In parallel, the AMPKα2 expression levels were all reduced by 60-80% compared with negative control group in AMPKα2 knockdown RAW264.7 cells ($P < 0.05$, 0.01 and 0.001). And their downstream signaling proteins were not regulated by Andro in AMPKα2-knockdown macrophages. These results suggest that AMPKα2 knockdown by siRNA significantly decreased the expression and activation of AMPKα (Fig. 6B and Fig. 7A). IKKα/β phosphorylation

was still suppressed by Andro but was not affected by AICAR in the presence of AMPKα2 siRNA. However, Andro could not inhibit the phosphorylation and degradation of lκBα in AMPKα2-knockdown macrophages (Fig. 6C and Fig. 7B). Moreover, the suppressive effects of Andro on the MAPK pathway were markedly abrogated by AMPKα2 knockdown (Fig. 6D and Fig. 7C). We next examined whether Andro inhibits NF-κB, p65 and AP-1 nuclear translocation in AMPKα2-knockdown macrophages. We found that the nuclear transcriptional activities of p65, p-c-Jun and c-Fos were not reduced by Andro after AMPKα2 knockdown (Fig. 8). These results unequivocally demonstrate that the anti-inflammatory effects of Andro depend on AMPK activation in LPS-induced macrophages.

3.7. Andro administration ameliorates DSS-induced acute colitis in mice

Based on the findings of our *in vitro* experiments, we next conducted *in vivo* studies by establishing a DSS-induced colitis model. To determine whether Andro relieves the symptoms of acute colitis in mice, the mouse disease activity index (DAI) was used for evaluation. As shown in Fig. 9A, the administration of Andro attenuated the loss of body weight. The DAI score of the Andro (100 mg/kg) treatment group was significantly lower than that of the DSS treatment group (Fig. 9C), and colon shortening was also significantly improved (Fig. 9B and D). H&E staining was used to observe colon histological damages, and the results showed that DSS treatment induced significant loss of colonic mucosa, glandular destruction or disappearance in the lamina propria, and decreased the expression of goblet cells and the infiltration of large numbers of inflammatory cells, but these histological changes were markedly attenuated in the Andro (100 mg/kg) treatment group (Fig. 10A). The IHC analysis demonstrated that CD68 and F4/80 macrophage infiltration was increased in the DSS treatment group, but in contrast, infiltration was decreased in the Andro (100 mg/kg) treatment group (Fig. 10B).

3.8. Andro suppresses the DSS-induced inflammatory response in acute colitis mice

model

To further demonstrate the anti-inflammatory effect of Andro *in vivo*, we detected proinflammatory cytokines in colon and spleen tissues of DSS-induced acute colitis model mice. Andro significantly reduced the mRNA levels of IL-6, TNF-α and IL-1β in colon tissues (Fig. 11A) while inhibiting the production of IL-6, TNF-α and IL-1β in spleen tissues (Fig. 11B). We next determined the phosphorylation levels of the AMPK, NF-κB and MAPK pathways by Western blotting. As expected, the results showed that Andro upregulated the phosphorylation of LKB1, AMPKα, ACC and GSK3β. In contrast, Andro markedly decreased the degradation of IκBα and the phosphorylation levels of IKK, IκBα, ERK, JNK, p38, mTOR and p70S6K in the intestinal tissues of DSS-induced acute colitis mice. These results indicate that Andro activates the AMPK (Fig. 12A and D) pathway and inhibits the NF-κB (Fig. 12B and E) and MAPK (Fig. 12C and F) pathways *in vivo*.

4. Discussion

For decades, previous studies have reported that Andro has anti-inflammatory effects in both *in vitro* and *in vivo* experimental inflammation models[1, 6, 39]. Andro and its derivatives downregulate adhesion molecules, proinflammatory cytokines, chemokines, lipid mediators and NO, mainly by inhibiting NF-κB activation[1, 39]. However, it is still unclear how Andro affects NF-κB or other signaling pathways to inhibit inflammation. Therefore, we confirmed the anti-inflammatory effects of Andro and explored its underlying mechanism in this study. We found that Andro inhibits inflammatory responses in LPS-induced macrophages via AMPK activation and improves DSS-induced acute colitis in mice.

Macrophages play a critical role in the inflammatory process[25]. When inflammation is triggered by pathogens, macrophages recognize different pathogen-associated molecular patterns (PAMPs) by TLR4, for example, LPS, lipoteichoic acid (LTA),

other viral proteins, etc., and when they bind to the TLR4 complex, the NF-κB and MAPK pathways are activated to promote the production of proinflammatory cytokines (IL-1β, IL-6, IL-8 and TNF-α). Furthermore, the upregulation of the reactive oxygen species (ROS), NO and prostaglandin (PG) E_2 lead to tissue damage and inflammation[27, 40, 41]. Our data showed that Andro not only inhibited the NF-κB and MAPK pathways but also affected their TLR4-mediated upstream signaling pathway and suppressed downstream proinflammatory reactions in 3 different macrophage cell lines. Therefore, our study strongly confirmed that Andro has anti-inflammatory effects in LPS-induced macrophages.

However, despite the continuous research, the pathway leading to the de-activation of these inflammatory signaling pathways by Andro was not fully revealed. Previous studies have shown that bacterial endotoxin such as LPS not only increases the release of pro-inflammatory cytokines but also induces apoptosis in the macrophages[42, 43]. In addition, LPS-induced macrophage activation triggers metabolic reprogramming through increased glucose uptake and glycosis, which is required for inflammatory response[44]. To find specific target genes and mechanisms of Andro, which affects the NF-κB/MAPK/TLR4-MyD88 pathways, we tested the effects of Andro on some specific marker proteins related to inflammation, metabolism, apoptosis, etc., in LPS-induced macrophages (Fig.6). We observed that Andro has the most obvious effect on the AMPK signaling pathway among the investigated other signaling pathways. Although the results of AMPK phosphorylation through intracellular signaling array contradict those obtained with Western blot analysis, AMPK activation by Andro was clearly demonstrated in subsequent experiments. Moreover, previous study has reported that Andro can activate LKB1-AMPK signaling pathway in human nasopharyngeal carcinoma (NPC) cell line, C666-1 cells[45]. Therefore, in this study, AMPK activation by Andro has been suggested as a therapeutic target in LPS-induced macrophages.

AMPK is a major cellular energy sensor that regulates metabolism in eukaryotes, and

is also a serine/threonine kinase that consists of a catalytic α subunit (α1 and α2) and regulatory β (β1 and β2) and γ (γ1, γ2 and γ3) subunits[38, 46]. The phosphorylation of the α subunit (Thr172) via several upstream kinases (LKB1, CaMKK) and allosteric regulation of increased AMP concentration lead to AMPK activation[47]. Accumulating research suggests that AMPK activation exerts anti-inflammatory effect in several immune cells including macrophage, neutrophils, T cells and mast cells[38, 48]. Yang Z, et al. reported that AMPK activation inhibited NF-κB activation, phosphorylation of the MAPK signaling pathway and the production of IL-1β, IL-6, iNOS, MCP-1 and COX-2 in LPS-induced macrophages[49, 50]. Likewise, our study demonstrated that Andro markedly upregulated the AMPK pathway, while it downregulated the NF-κB and MAPK pathways.

The catalytic subunit of AMPK complexes has two isoforms, α1 and α2. The activation of the AMPKα2 isoform inhibited IKK phosphorylation and IκBα degradation in endothelial cells (ECs) from AMPKα2$^{+/+}$ but not in ECs from AMPKα2$^{-/-}$ mice[51]. AMPKα2 was also reported that its activation directly interact with TAK1 and inhibit TAK1-dependent MAPK signaling cascade in J774 macrophages[50]. ERK1/2 inhibitor couldn't regulate FcεRI-dependent mast cell activation and anaphylaxis following AMPKα2 knockdown[52]. Thus, we demonstrated the association between AMPK activation and the NF-κB/MAPK signaling pathways by using AMPKα2 siRNA silencing. Interestingly, we found that Andro could not regulate AMPK/NF-κB/MAPK pathways, NF-κB and AP-1 nuclear translocation and NO production following AMPKα2 knockdown but still affected the phosphorylation of IKK and LKB1. Previous reports showed that AICAR-mediated AMPK activation didn't have inhibitory effect on the phosphorylation of IKK in LPS-induced macrophages[53], but Bess *et al.* reported that IKK is a direct substrate of AMPKα2 in ECs[51]. The role of AMPK in the IKK phosphorylation is complicated and suggested that it's mechanisms may be depended on certain cell type[54]. Overall, our results indicated that Andro inhibits NF-κB activation and the MAPK signaling pathway as well as the downstream

proinflammatory response initiated by AMPK activation in LPS-induced macrophages.

DSS is a synthetic chemical substance consisting of sulfated polysaccharide that chemically damages the intestinal tract and causes an increase in bacterial invasion. In the DSS-induced mice colitis model, DSS administration leads to body weight loss, changes in stool consistency, rectal bleeding and histological damages including intestinal goblet cell and mucin depletion, mucosal epithelial erosion and/or ulceration, and an influx of immune cells in the lamina propria and submucosa, hereby inducing immune responses[34, 55]. Moreover, previous studies have shown that the DSS-induced mice colitis model resembles the clinical and histological features of human UC[56]. Our data showed that Andro significantly attenuated DSS-induced pathological changes and histological damages. Andro was also reported to inhibit Th1/Th17 response and promote Th2 response in the peripheral blood mononuclear cells (PBMCs) which were isolated from UC patients[22]. IL-23, which promote Th1/Th17 response, is induced by lamina propria macrophages in the IBD[57]. Macrophages are regarded as crucial components of protective immunity and are involved in the pathology of IBD but also maintain mucosal homeostasis with the microbiota and contribute to epithelial renewal[26, 27]. Moreover, bacteria are recognized by TLR4 on macrophages in the intestine, thereby activating the NF-κB and MAPK signaling pathways, which produce a variety of proinflammatory cytokines and chemokines[26, 58-61]. We demonstrated that Andro reduced the production of proinflammatory cytokines by inhibiting the activation of the NF-κB and MAPK signaling pathways *in vivo*.

In recent years, emerging evidence indicates that AMPK activation may act as a central therapeutic target in the inflammatory response of murine colitis. AICAR, an agonist of AMPK, not only activated AMPK, but also inhibited NF-κB activation and expression levels of Th1- and Th17- type cytokines in acute and chronic experimental colitis[62]. The treatments with metformin, eupatilin, 6-gingerol, etc. were showed to ameliorate DSS-induced mice colitis by suppressing proinflammatory cytokines and improving intestinal epithelial barrier dysfunction by activating AMPK[63-65]. Here, we

showed that Andro activates the AMPK pathway and reduced the downstream proinflammatory response in DSS-induced colitis mice; these results suggest that Andro treatment exerts anti-inflammatory effects on experimental colitis through AMPK activation.

In summary, the findings of this study provide new insight into the anti-inflammatory mechanism of Andro which inhibits inflammatory responses through AMPK activation *in vitro* and *in vivo*, and the scientific basis for future anti-inflammatory drug development for IBD treatment.

Conflict of interest

The authors declare that there are no conflicts of interest.

Acknowledgements

This work was financially sponsored by the National Natural Science Foundation of China (NSFC) Grants 81803545.

References

[1] W.S.D. Tan, W. Liao, S. Zhou, W.S.F. Wong, Is there a future for andrographolide to be an anti-inflammatory drug? Deciphering its major mechanisms of action, Biochemical pharmacology 139 (2017) 71-81. doi:10.1016/j.bcp.2017.03.024

[2] O. Sareer, S. Ahmad, S. Umar, Andrographis paniculata: a critical appraisal of extraction, isolation and quantification of andrographolide and other active constituents, Natural Product Research 28(23) (2014) 2081-2101. doi:10.1080/14786419.2014.924004

[3] T. Zhu, W. Zhang, M. Xiao, H. Chen, H. Jin, Protective role of andrographolide in bleomycin-induced pulmonary fibrosis in mice, International journal of molecular sciences 14(12) (2013) 23581-96. doi:10.3390/ijms141223581

[4] W.S. Tan, H.Y. Peh, W. Liao, C.H. Pang, T.K. Chan, S.H. Lau, V.T. Chow, W.S. Wong, Cigarette Smoke-Induced Lung Disease Predisposes to More Severe Infection with Nontypeable Haemophilus influenzae: Protective Effects of Andrographolide, Journal of natural products 79(5) (2016) 1308-15. doi:10.1021/acs.jnatprod.5b01006

[5] S. Gupta, K.P. Mishra, L. Ganju, Broad-spectrum antiviral properties of andrographolide, Archives of virology 162(3) (2017) 611-623. doi:10.1007/s00705-016-3166-3

[6] Y. Dai, S.R. Chen, L. Chai, J. Zhao, Y. Wang, Y. Wang, Overview of pharmacological activities of Andrographis paniculata and its major compound andrographolide, Critical reviews in food science and nutrition 59(sup1) (2019) S17-s29. doi:10.1080/10408398.2018.1501657

[7] A. Banerjee, V. Banerjee, S. Czinn, T. Blanchard, Increased reactive oxygen species levels cause ER stress and cytotoxicity in andrographolide treated colon cancer cells, Oncotarget 8(16) (2017) 26142-26153. doi:10.18632/oncotarget.15393

[8] W. Wang, W. Guo, L. Li, Z. Fu, W. Liu, J. Gao, Y. Shu, Q. Xu, Y. Sun, Y. Gu, Andrographolide reversed 5-FU resistance in human colorectal cancer by elevating BAX expression, Biochemical pharmacology 121 (2016) 8-17. doi:10.1016/j.bcp.2016.09.024

[9] S. Kumar, H.S. Patil, P. Sharma, D. Kumar, S. Dasari, V.G. Puranik, H.V. Thulasiram, G. C. Kundu, Andrographolide inhibits osteopontin expression and breast tumor growth through down regulation of PI3 kinase/Akt signaling pathway, Current molecular medicine 12(8) (2012) 952-66.

[10] M.T. Islam, E.S. Ali, S.J. Uddin, M.A. Islam, S. Shaw, I.N. Khan, S.S.S. Saravi, S. Ahmad, S. Rehman, V.K. Gupta, M.A. Gaman, A.M. Gaman, S. Yele, A.K. Das, E.S.J.M. de Castro, S.M.M. de Moura Dantas, H.M.L. Rolim, A.A. de Carvalho Melo-Cavalcante, M.S. Mubarak, N.S. Yarla, J.A. Shilpi, S.K. Mishra, A.G. Atanasov, M.A. Kamal, Andrographolide, a diterpene lactone from Andrographis paniculata and its therapeutic promises in cancer, Cancer letters 420 (2018) 129-145. doi:10.1016/j.canlet.2018.01.074

[11] C.H. Yang, T.L. Yen, C.Y. Hsu, P.A. Thomas, J.R. Sheu, T. Jayakumar, Multi-Targeting Andrographolide, a Novel NF-kappaB Inhibitor, as a Potential Therapeutic Agent for Stroke, International journal of molecular sciences 18(8) (2017). doi:10.3390/ijms18081638

[12] Z. Zhu, H. Duan, M. Jing, L. Xu, P. Yu, Synthesis and Biological Evaluation of Andrographolide Derivatives as Anti-inflammatory Agent, Current pharmaceutical design 24(30) (2018) 3529-3533. doi:10.2174/1381612824666180724130014

[13] V. Kishore, N.S. Yarla, A. Bishayee, S. Putta, R. Malla, N.R. Neelapu, S. Challa, S. Das, Y. Shiralgi, G. Hegde, B.L. Dhananjaya, Multi-targeting Andrographolide and its Natural Anal

ogs as Potential Therapeutic Agents, Current topics in medicinal chemistry 17(8) (2017) 845-857. doi:10.2174/1568026616666160927150452

[14] S. Chakraborty, I. Ehsan, B. Mukherjee, L. Mondal, S. Roy, K.D. Saha, B. Paul, M.C. Debnath, T. Bera, Therapeutic potential of andrographolide-loaded nanoparticles on a murine asthma model, Nanomedicine : nanotechnology, biology, and medicine 20 (2019) 102006. doi:10.1016/j.nano.2019.04.009

[15] J. Li, L. Luo, X. Wang, B. Liao, G. Li, Inhibition of NF-kappaB expression and allergen-induced airway inflammation in a mouse allergic asthma model by andrographolide, Cellular & molecular immunology 6(5) (2009) 381-5. doi:10.1038/cmi.2009.49

[16] S. Peng, J. Gao, W. Liu, C. Jiang, X. Yang, Y. Sun, W. Guo, Q. Xu, Andrographolide ameliorates OVA-induced lung injury in mice by suppressing ROS-mediated NF-kappaB signaling and NLRP3 inflammasome activation, Oncotarget 7(49) (2016) 80262-80274. doi:10.18632/oncotarget.12918

[17] H. Xia, J. Xue, H. Xu, M. Lin, M. Shi, Q. Sun, T. Xiao, X. Dai, L. Wu, J. Li, Q. Xiang, H. Tang, Q. Bian, Q. Liu, Andrographolide antagonizes the cigarette smoke-induced epithelial-mesenchymal transition and pulmonary dysfunction through anti-inflammatory inhibiting HOTAIR, Toxicology 422 (2019) 84-94. doi:10.1016/j.tox.2019.05.009

[18] W.S.D. Tan, W. Liao, H.Y. Peh, M. Vila, J. Dong, H.M. Shen, W.S.F. Wong, Andrographolide simultaneously augments Nrf2 antioxidant defense and facilitates autophagic flux blockade in cigarette smoke-exposed human bronchial epithelial cells, Toxicology and applied pharmacology 360 (2018) 120-130. doi:10.1016/j.taap.2018.10.005

[19] S.P. Guan, W. Tee, D.S. Ng, T.K. Chan, H.Y. Peh, W.E. Ho, C. Cheng, J.C. Mak, W.S. Wong, Andrographolide protects against cigarette smoke-induced oxidative lung injury via augmentation of Nrf2 activity, British journal of pharmacology 168(7) (2013) 1707-18. doi:10.1111/bph.12054

[20] J.C. Lee, C.K. Tseng, K.C. Young, H.Y. Sun, S.W. Wang, W.C. Chen, C.K. Lin, Y.H. Wu, Andrographolide exerts anti-hepatitis C virus activity by up-regulating haeme oxygenase-1 via the p38 MAPK/Nrf2 pathway in human hepatoma cells, British journal of pharmacology 171(1) (2014) 237-52. doi:10.1111/bph.12440

[21] B.J. Guo, Z. Liu, M.Y. Ding, F. Li, M. Jing, L.P. Xu, Y.Q. Wang, Z.J. Zhang, Y. Wang, D. Wang, G.C. Zhou, Y. Wang, Andrographolide derivative ameliorates dextran sulfate sodium-induced experimental colitis in mice, Biochemical pharmacology 163 (2019) 416-424. doi:10.1016/j.bcp.2019.03.019

[22] Q. Zhu, P. Zheng, J. Zhou, X. Chen, Y. Feng, W. Wang, F. Zhou, Q. He, Andrographolide affects Th1/Th2/Th17 responses of peripheral blood mononuclear cells from ulcerative colitis patients, Molecular medicine reports 18(1) (2018) 622-626. doi:10.3892/mmr.2018.8992

[23] Q. Zhu, P. Zheng, X. Chen, F. Zhou, Q. He, Y. Yang, Andrographolide presents therapeutic effect on ulcerative colitis through the inhibition of IL-23/IL-17 axis, American journal of translational research 10(2) (2018) 465-473.

[24] Z. Gao, C. Yu, H. Liang, X. Wang, Y. Liu, X. Li, K. Ji, H. Xu, M. Yang, K. Liu, D. Qi, H. Fan, Andrographolide derivative CX-10 ameliorates dextran sulphate sodium-induced ulcerative colitis in mice: Involvement of NF-kappaB and MAPK signalling pathways, Internationa

l immunopharmacology 57 (2018) 82-90. doi:10.1016/j.intimp.2018.02.012

[25] N. Fujiwara, K. Kobayashi, Macrophages in inflammation, Current drug targets. Inflammation and allergy 4(3) (2005) 281-6. doi:10.2174/1568010054022024

[26] C.C. Bain, A.M. Mowat, Macrophages in intestinal homeostasis and inflammation, Immunological reviews 260(1) (2014) 102-17. doi:10.1111/imr.12192

[27] Y.R. Na, M. Stakenborg, S.H. Seok, G. Matteoli, Macrophages in intestinal inflammation and resolution: a potential therapeutic target in IBD, Nature reviews. Gastroenterology & hepatology (2019). doi:10.1038/s41575-019-0172-4

[28] D. Lissner, M. Schumann, A. Batra, L.I. Kredel, A.A. Kuhl, U. Erben, C. May, J.D. Schulzke, B. Siegmund, Monocyte and M1 Macrophage-induced Barrier Defect Contributes to Chronic Intestinal Inflammation in IBD, Inflammatory bowel diseases 21(6) (2015) 1297-305. doi:10.1097/mib.0000000000000384

[29] C. Fiocchi, Inflammatory bowel disease pathogenesis: where are we?, Journal of gastroenterology and hepatology 30 Suppl 1 (2015) 12-8. doi:10.1111/jgh.12751

[30] G.G. Kaplan, The global burden of IBD: from 2015 to 2025, Nature reviews. Gastroenterology & hepatology 12(12) (2015) 720-7. doi:10.1038/nrgastro.2015.150

[31] K. Fellermann, Adverse events of tumor necrosis factor inhibitors, Digestive diseases (Basel, Switzerland) 31(3-4) (2013) 374-8. doi:10.1159/000354703

[32] C.P. Bauerfeld, R. Rastogi, G. Pirockinaite, I. Lee, M. Huttemann, B. Monks, M.J. Birnbaum, L. Franchi, G. Nunez, L. Samavati, TLR4-mediated AKT activation is MyD88/TRIF dependent and critical for induction of oxidative phosphorylation and mitochondrial transcription factor A in murine macrophages, Journal of immunology (Baltimore, Md. : 1950) 188(6) (2012) 2847-57. doi:10.4049/jimmunol.1102157

[33] Y. Lu, S.J. Suh, C.H. Kwak, K.M. Kwon, C.S. Seo, Y. Li, Y. Jin, X. Li, S.L. Hwang, O. Kwon, Y.C. Chang, Y.G. Park, S.S. Park, J.K. Son, C.H. Kim, H.W. Chang, Saucerneol F, a new lignan, inhibits iNOS expression via MAPKs, NF-kappaB and AP-1 inactivation in LPS-induced RAW264.7 cells, International immunopharmacology 12(1) (2012) 175-81. doi:10.1016/j.intimp.2011.11.008

[34] B. Chassaing, J.D. Aitken, M. Malleshappa, M. Vijay-Kumar, Dextran sulfate sodium (DSS)-induced colitis in mice, Current protocols in immunology 104 (2014) Unit 15.25. doi:10.1002/0471142735.im1525s104

[35] H.S. Cooper, S.N. Murthy, R.S. Shah, D.J. Sedergran, Clinicopathologic study of dextran sulfate sodium experimental murine colitis, Laboratory investigation; a journal of technical methods and pathology 69(2) (1993) 238-49.

[36] C. Qu, Z.W. Yuan, X.T. Yu, Y.F. Huang, G.H. Yang, J.N. Chen, X.P. Lai, Z.R. Su, H.F. Zeng, Y. Xie, X.J. Zhang, Patchouli alcohol ameliorates dextran sodium sulfate-induced experimental colitis and suppresses tryptophan catabolism, Pharmacological research 121 (2017) 70-82. doi:10.1016/j.phrs.2017.04.017

[37] Y. Lu, N.M. Kim, Y.W. Jiang, H. Zhang, D. Zheng, F.X. Zhu, R. Liang, B. Li, H.X. Xu, Cambogin suppresses dextran sulphate sodium-induced colitis by enhancing Treg cell stability and function, 175(7) (2018) 1085-1099. doi:10.1111/bph.14150

[38] E.A. Day, R.J. Ford, G.R. Steinberg, AMPK as a Therapeutic Target for Treating Metabol

ic Diseases, Trends in endocrinology and metabolism: TEM 28(8) (2017) 545-560. doi:10.1016/j.tem.2017.05.004

[39] J.C. Lim, T.K. Chan, D.S. Ng, S.R. Sagineedu, J. Stanslas, W.S. Wong, Andrographolide and its analogues: versatile bioactive molecules for combating inflammation and cancer, Clinical and experimental pharmacology & physiology 39(3) (2012) 300-10. doi:10.1111/j.1440-1681.2011.05633.x

[40] V. Kumar, A.K. Abbas, J.C. Aster, S.L. Robbins, Robbins basic pathology, Elsevier/Saunders, Philadelphia, PA, 2013.

[41] S.K. Biswas, A. Mantovani, Macrophage plasticity and interaction with lymphocyte subsets: cancer as a paradigm, Nat Immunol 11(10) (2010) 889-96. doi:10.1038/ni.1937

[42] Y. Wang, X. Mao, H. Chen, J. Feng, M. Yan, Y. Wang, Y. Yu, Dexmedetomidine alleviates LPS-induced apoptosis and inflammation in macrophages by eliminating damaged mitochondria via PINK1 mediated mitophagy, International immunopharmacology 73 (2019) 471-481. doi:10.1016/j.intimp.2019.05.027

[43] X. Luo, H. Zhang, X. Wei, M. Shi, P. Fan, W. Xie, Y. Zhang, N. Xu, Aloin Suppresses Lipopolysaccharide-Induced Inflammatory Response and Apoptosis by Inhibiting the Activation of NF-kappaB, Molecules (Basel, Switzerland) 23(3) (2018). doi:10.3390/molecules23030517

[44] C. Diskin, E.M. Palsson-McDermott, Metabolic Modulation in Macrophage Effector Function, Frontiers in immunology 9 (2018) 270. doi:10.3389/fimmu.2018.00270

[45] B. Wu, X. Chen, Y. Zhou, P. Hu, D. Wu, G. Zheng, Y. Cai, Andrographolide inhibits proliferation and induces apoptosis of nasopharyngeal carcinoma cell line C666-1 through LKB1-AMPK-dependent signaling pathways, Die Pharmazie 73(10) (2018) 594-597. doi:10.1691/ph.2018/8583

[46] D.G. Hardie, AMPK--sensing energy while talking to other signaling pathways, Cell metabolism 20(6) (2014) 939-52. doi:10.1016/j.cmet.2014.09.013

[47] S. Herzig, R.J. Shaw, AMPK: guardian of metabolism and mitochondrial homeostasis, Nature reviews. Molecular cell biology 19(2) (2018) 121-135. doi:10.1038/nrm.2017.95

[48] J. Wang, Z. Li, L. Gao, Y. Qi, H. Zhu, X. Qin, The regulation effect of AMPK in immune related diseases, Science China. Life sciences 61(5) (2018) 523-533. doi:10.1007/s11427-017-9169-6

[49] H.W. Jeong, K.C. Hsu, J.W. Lee, M. Ham, J.Y. Huh, H.J. Shin, W.S. Kim, J.B. Kim, Berberine suppresses proinflammatory responses through AMPK activation in macrophages, American journal of physiology. Endocrinology and metabolism 296(4) (2009) E955-64. doi:10.1152/ajpendo.90599.2008

[50] M.Y. Chang, F.M. Ho, J.S. Wang, H.C. Kang, Y. Chang, Z.X. Ye, W.W. Lin, AICAR induces cyclooxygenase-2 expression through AMP-activated protein kinase-transforming growth factor-beta-activated kinase 1-p38 mitogen-activated protein kinase signaling pathway, Biochemical pharmacology 80(8) (2010) 1210-20. doi:10.1016/j.bcp.2010.06.049

[51] E. Bess, B. Fisslthaler, T. Fromel, I. Fleming, Nitric oxide-induced activation of the AMP-activated protein kinase alpha2 subunit attenuates IkappaB kinase activity and inflammatory responses in endothelial cells, PloS one 6(6) (2011) e20848. doi:10.1371/journal.pone.0020848

[52] S.L. Hwang, Y. Lu, X. Li, Y.D. Kim, Y.S. Cho, Y. Jahng, J.K. Son, Y.J. Lee, W. Kang,

Y. Taketomi, M. Murakami, T.C. Moon, H.W. Chang, ERK1/2 antagonize AMPK-dependent r egulation of FcepsilonRI-mediated mast cell activation and anaphylaxis, The Journal of allergy and clinical immunology 134(3) (2014) 714-721.e7. doi:10.1016/j.jaci.2014.05.001

[53] Z. Yang, B.B. Kahn, H. Shi, B.Z. Xue, Macrophage alpha1 AMP-activated protein kinase (alpha1AMPK) antagonizes fatty acid-induced inflammation through SIRT1, The Journal of biol ogical chemistry 285(25) (2010) 19051-9. doi:10.1074/jbc.M110.123620

[54] I.P. Salt, T.M. Palmer, Exploiting the anti-inflammatory effects of AMP-activated protein kinase activation, Expert opinion on investigational drugs 21(8) (2012) 1155-67. doi:10.1517/13 543784.2012.696609

[55] P. Kiesler, I.J. Fuss, W. Strober, Experimental Models of Inflammatory Bowel Diseases, Cellular and molecular gastroenterology and hepatology 1(2) (2015) 154-170. doi:10.1016/j.jcmg h.2015.01.006

[56] D.D. Eichele, K.K. Kharbanda, Dextran sodium sulfate colitis murine model: An indispens able tool for advancing our understanding of inflammatory bowel diseases pathogenesis, World journal of gastroenterology 23(33) (2017) 6016-6029. doi:10.3748/wjg.v23.i33.6016

[57] M. Sarra, F. Pallone, T.T. Macdonald, G. Monteleone, IL-23/IL-17 axis in IBD, Inflamma tory bowel diseases 16(10) (2010) 1808-13. doi:10.1002/ibd.21248

[58] M.H. Zaki, M. Lamkanfi, T.D. Kanneganti, The Nlrp3 inflammasome: contributions to inte stinal homeostasis, Trends in immunology 32(4) (2011) 171-9. doi:10.1016/j.it.2011.02.002

[59] M.P. Wymann, M. Zvelebil, M. Laffargue, Phosphoinositide 3-kinase signaling-Which way to target?, Trends in Pharmacological Sciences 24(7) (2003) 366-376. doi:10.1016/S0165-6147(0 3)00163-9

[60] N. Goyal, A. Rana, A. Ahlawat, K.R. Bijjem, P. Kumar, Animal models of inflammatory bowel disease: a review, Inflammopharmacology 22(4) (2014) 219-33. doi:10.1007/s10787-014-0 207-y

[61] R. Dheer, R. Santaolalla, J.M. Davies, J.K. Lang, M.C. Phillips, C. Pastorini, M.T. Vazqu ez-Pertejo, M.T. Abreu, Intestinal Epithelial Toll-Like Receptor 4 Signaling Affects Epithelial F unction and Colonic Microbiota and Promotes a Risk for Transmissible Colitis, Infection and i mmunity 84(3) (2016) 798-810. doi:10.1128/iai.01374-15

[62] A. Bai, M. Yong, A.G. Ma, Y. Ma, C.R. Weiss, Q. Guan, C.N. Bernstein, Z. Peng, Nov el anti-inflammatory action of 5-aminoimidazole-4-carboxamide ribonucleoside with protective ef fect in dextran sulfate sodium-induced acute and chronic colitis, The Journal of pharmacology and experimental therapeutics 333(3) (2010) 717-25. doi:10.1124/jpet.109.164954

[63] L. Chen, J. Wang, Q. You, S. He, Q. Meng, J. Gao, X. Wu, Y. Shen, Y. Sun, X. Wu, Q. Xu, Activating AMPK to Restore Tight Junction Assembly in Intestinal Epithelium and to Attenuate Experimental Colitis by Metformin, Frontiers in pharmacology 9 (2018) 761. doi:10.3 389/fphar.2018.00761

[64] K. Zhou, R. Cheng, B. Liu, L. Wang, H. Xie, C. Zhang, Eupatilin ameliorates dextran su lphate sodium-induced colitis in mice partly through promoting AMPK activation, Phytomedicin e : international journal of phytotherapy and phytopharmacology 46 (2018) 46-56. doi:10.1016/j. phymed.2018.04.033

[65] K.W. Chang, C.Y. Kuo, 6-Gingerol modulates proinflammatory responses in dextran sodiu

m sulfate (DSS)-treated Caco-2 cells and experimental colitis in mice through adenosine monop hosphate-activated protein kinase (AMPK) activation, Food & function 6(10) (2015) 3334-41. d oi:10.1039/c5fo00513b

Figure Legends

Fig. 1 Effects of Andro on the production of NO and proinflammatory cytokines in LPS-induced macrophages. RAW264.7 cells were treated with Andro at different concentrations ranging from 1 to 100 μM for 24 h, and cell viability (A) was determined by the MTT assay. The cells were pretreated with Andro (1, 10 μM) for 1 h, followed by treatment with LPS (1 μg/mL) for 6 h (for PCR), 12 h (for ELISA) and 24 h (for the Griess assay and Western blot analysis). BMDMs were pretreated with Andro (1, 10 μM) for 1 h, followed by treatment with LPS (10 μg/mL)+IFN-γ (20 ng/ml) for 24 h (for the Griess assay and Western blot analysis). NO production (B and C) was measured by the Griess assay. The protein levels of iNOS and COX-2 (D and E) were detected by Western blot analysis and normalized to that of β-actin by using ImageJ software. The production (F) of IL-6, TNF-α and IL-1β was measured by ELISA, and their mRNA levels (G) were detected by PCR. All results are shown as the mean ± SD of three independent experiments. ## $P < 0.01$, ### $P < 0.001$, compared to the nontreated group. * $P < 0.05$, ** $P < 0.01$, *** $P < 0.001$, compared to the LPS-treated group.

Fig. 2 Effects of Andro on the NF-κB/MAPK/TLR4-MyD88 signaling pathways in LPS-induced macrophages. RAW264.7 (A) and BMDM (B) cells were pretreated with Andro (1, 10 μM) for 1 h, followed by treatment with LPS (1 μg/mL) or LPS(10 μg/mL)+IFN-γ (20 ng/ml) for 15 min or 30 min. The proteins levels of the NF-κB/MAPK/TLR4-MyD88 pathways were determined by Western blot analysis and normalized to β-actin or total protein by using ImageJ software. The results are shown in the bar graphs as the mean ± SD. # $P < 0.05$, ## $P < 0.01$, ### $P < 0.001$, compared to the nontreated group. * $P < 0.05$, ** $P < 0.01$, *** $P < 0.001$, compared to the LPS-treated group.

Fig. 3 Effects of Andro on NF-κB p65 and AP-1 nuclear translocation in LPS-induced RAW264.7 cells. RAW264.7 cells were pretreated with Andro (1, 10 μM) for 1 h, followed by treatment with LPS (1 μg/mL) for 30 min. The protein levels of p65, p-c-Jun and c-Fos in the cytosolic and nuclear fractions were determined by Western blot analysis (A) and normalized to β-tubulin or Lamin A+C by using ImageJ software. The cellular localizations of p65, p-c-Jun and c-Fos were analyzed using IF staining (B). Nuclei were stained with DAPI. All of the experiments were performed at least three times. The Western blot results are shown in the bar graphs as the mean ± SD. # $P < 0.05$, ## $P < 0.01$, ### $P < 0.001$, compared to the nontreated group. * $P < 0.05$, ** $P < 0.01$, *** $P < 0.001$, compared to the LPS-treated group.

Fig. 4 Effects of Andro on the phosphorylation and activation of the indicated cellular proteins in LPS-induced macrophages. Representative chemiluminescent array images of the PathScan Intracellular Signaling Array Kit (A) and heat map (B) show various phosphorylated signaling nodes in LPS and IFN-γ-induced BMDMs. RAW264.7 cells were pre-treated with Andro (1, 10 μM) for 1 h, followed by stimulation with LPS (1 μg/mL) for 15 min (C) and 12 h (D). The proteins levels were determined by Western blot analysis and normalized to β-actin. The Western blot results are shown in the bar graphs as the mean ± SD. # $P < 0.05$, ## $P < 0.01$, ### $P < 0.001$, compared to the nontreated group. * $P < 0.05$, ** $P < 0.01$, *** $P < 0.001$, compared to the LPS-treated group.

Fig. 5 Comparison of the effects of Andro with AICAR and Compound C in LPS-induced RAW264.7 cells. RAW264.7 cells were pretreated with Andro (10 μM) and Compound C (10 μM) for 1 h and with AICAR (1 mM) for 4 h, followed by treatment with LPS (1 μg/mL) for 15 min (A, B) or 30 min (C). The proteins levels of the AMPK (A)/NF-κB (B)/MAPK (C) pathways were determined by Western blot analysis and

normalized to β-actin by using ImageJ software. All results are representative as the mean ± SD. # $P < 0.05$, ## $P < 0.01$, ### $P < 0.001$, compared to the nontreated group. * $P < 0.05$, ** $P < 0.01$, *** $P < 0.001$, compared to the LPS-treated group.

Fig. 6 Effects of Andro on the LPS-induced NO production and inflammatory signaling pathways following knockdown of AMPKα2. RAW264.7 cells were transfected with negative control siRNA or AMPKα2 siRNA for 48 h. Transfected cells were pretreated with Andro (10 μM) for 1 h and with AICAR (1 mM) for 4 h, followed by treatment with LPS (1 μg/mL) for 15 min (B, C), 30 min (D) and 24 h (A). Then, the production of NO was evaluated by the Griess assay (A), and the phosphorylation of the AMPK (B)/NF-κB (C)/MAPK (D) pathways was detected by Western blot analysis. The Griess assay result was presented as the mean ± SD. *$P < 0.05$, ***$P < 0.001$, compared to the negative control group; # $P < 0.05$, compared to the nontreated group.

Fig. 7 Relative protein levels of the AMPK/NF-κB/MAPK pathways following knockdown of AMPKα2. The protein levels of the AMPK (A)/NF-κB (B)/MAPK (C) pathways in LPS-induced AMPKα2-knockdown macrophages were detected by Western blot analysis and normalized to β-actin by using ImageJ software. All of the Western blot results were presented as the mean ± SD. * $P < 0.05$, ** $P < 0.01$, *** $P < 0.001$, compared to the negative control group.

Fig. 8 Effects of Andro on NF-κB p65 and AP-1 nuclear translocation following knockdown of AMPKα2. The AMPKα2 gene in RAW264.7 cells was silenced by siRNA transfection, RAW264.7 cells were pre-treated with andrographolide (10 μM) for 1 h and AICAR (1 mM) for 4 h, followed by stimulation with LPS (1 μg/mL) for 30 min, and then the cellular localizations of p65, p-c-Jun and c-Fos were analyzed by

IF. Nuclei were stained with DAPI.

Fig. 9 Effects of Andro on DSS-induced acute colitis in mice. Acute colitis was induced in BALB/c mice (n=4-5/group) by orally administering 3.5% DSS in drinking water from day 0 to day 7. Mice received Andro (50 and 100 mg/kg) and SASP (200 mg/kg) treatment each day from day 1 to day 7. Body weight changes (A) and DAI (C) were measured every day from day 0. The length (B) and macroscopic appearances (D) of colon length were measured after the mice had been sacrificed on day 8. All data are presented as the mean ± SD. Compared with the normal control group, #$P < 0.05$, ## $P < 0.01$, ### $P < 0.001$; compared with the DSS control group, *** $P < 0.001$; the Andro (50 mg/kg) treatment group compared with the DSS control group, ▲ $P < 0.05$; the Andro (100 mg/kg) treatment group compared with the DSS control group, ▼ $P < 0.05$; the SASP treatment group compared with the DSS control group, ♦ $P < 0.05$, ♦♦ $P < 0.01$.

Fig. 10 Effects of Andro on histological changes and macrophage infiltration in the colon tissue. Colorectal histologic changes were determined by H&E staining (A), and the infiltration of F4/80 and CD68 macrophages was examined by IHC (B). The quantification of integrated OD (IOD) in each group was analyzed by Image Pro-Plus 6.0. All data are representative as the mean ± SD. Compared with the normal control group, ## $P < 0.01$, ### $P < 0.001$; compared with the DSS control group, ** $P < 0.01$, *** $P < 0.001$.

Fig. 11 Effects of Andro on the mRNA expression and the production of proinflammatory cytokines *in vivo*. The mRNA levels of IL-6, TNF-α and IL-1β in the colon tissue were detected by PCR (A). The production of IL-6, TNF-α and IL-1β in

the spleen tissue of DSS-induced acute colitis was measured by ELISA (B). All results are shown as the mean ± SD. # $P < 0.01$, ## $P < 0.01$, ### $P < 0.001$, compared to the normal control group. * $P < 0.05$, ** $P < 0.01$, *** $P < 0.001$, compared to the DSS control group.

Fig. 12 Effects of Andro on the activation of the AMPK/NF-κB/MAPK pathways *in vivo*. The phosphorylation levels of the AMPK (A, D), NF-κB (B, E) and MAPK (C, F) pathways were detected by Western blot analysis and normalized to β-actin by using ImageJ software. The Western blot results are shown in the bar graphs. All results are shown as the mean ± SD. ## $P < 0.01$, ### $P < 0.001$, compared to the normal control group. * $P < 0.05$, ** $P < 0.01$, *** $P < 0.001$, compared DSS control group.